

# Mechanical analysis of concrete structures submitted to an aggressive water attack

C.Le Bellégo & B.Gérard

*Electricité de France, Research and development Division, department MTC, France  
LMT Cachan, ENS Cachan / CNRS / Université Paris VI, France*

G.Pijaudier-Cabot

*R&DO, Laboratoire de Génie Civil de Nantes-Saint Nazaire, Ecole Centrale de Nantes, Nantes, France*

**ABSTRACT** : Long term durability of concrete structures, some waste disposals especially, is a problem which must be faced both from the point of view of cracking and physical degradations. In this contribution, we investigate the case of leaching of concrete structures as an example. There are two sources of material damage: one which is due to mechanical actions, and a second one which is due to an increase of material porosity as several of its components are being dissolved. Experimental data aimed at exhibiting the influence of chemical damage on the fracture properties of the material are discussed first. Size effect tests, at various levels of calcium leaching, have been performed on mortar beam. The beams have been leached first and then they are loaded in order to obtain their residual strength. The experiments show that the stiffness and maximum loads are decreased upon leaching. The brittleness of the structures is increased and the fracture energy decreases. Then, we examine the relevance of an existing constitutive relation aimed at modelling mechanical and chemical damage. The interpretation of the size effect tests shows that the mechanical internal length of the material cannot be considered as a constant in the presence of chemical damage.

## 1. INTRODUCTION

Reliable predictions of the long-term behaviour of concrete structures require a sound knowledge of the various degradation mechanisms that affect the structures over their life-time, and the extensive use of simulation tools. One of the main mechanisms of degradation is leaching due to aggressive water and particularly calcium leaching as calcium is the most important element in the hydrated cement paste. The main consequences on the cement paste microstructure are an increase of porosity and a decrease of the mechanical properties of the material with time: a loss of elastic properties and a loss of strength [3,4]. This chemical degradation mechanism must be superimposed to mechanical damage and experiments must be devised in order to calibrate model parameters. As leaching is a very slow process, accelerated procedures are needed: ammonium nitrate has been chosen by few authors as a representative aggressive solution. For example, Goncalves and Rodrigues [6] have studied, for 14 years, the influence of calcium leaching on the residual strength of beams for different cements. Schneider [13, 14] has performed experiments on beams subjected to different aggressive solutions

and has shown that there is a decrease of maximal strength with time.

Different models have been developed to describe all these coupling effects. A model developed by Gerard [4,5] uses a finite element analysis coupling leaching and a non-local damage model [9, 11]. It is based on the definition of two damage variables: one is due to mechanical loads and the other one, which could be called an ageing variable, accounts for chemical damage. The model can provide predictions of the residual strength and of the life-time of concrete structures subjected to aggressive water. Its range of validity needs, however, to be explored.

After a brief review of the mechanisms involved in the chemical damage process, we present size effect experiments aimed at exhibiting the variation of fracture energy due to chemical damage. Then, the constitutive relation due to Gérard and its calibration are discussed. Comparisons with the size effect tests data are performed.

## 2. CALCIUM LEACHING OF CEMENT-BASED MATERIALS

Concrete is a reactive porous material. Hydrates and

water are the main components of the binder. Solid phases are in thermodynamic equilibrium with the surrounding pore solution chemistry. The calcium is the main chemical component of the binder.

The hydrates leaching process is essentially caused by the difference of composition and chemical activity between water in contact with concrete and the pore solution inside concrete. The difference between the pore solution and the external solution causes the motion of ions out of the cement paste. This overall motion of ions breaks the thermodynamic equilibrium established between the pore solution and the hydration products, and favours the dissolution of solids phases such as portlandite and C-S-H. Figure 1 shows the equilibrium diagram between the calcium in the solid phase C (divided by the amount of silica S) and the calcium in the liquid phase  $Ca^{++}$ .

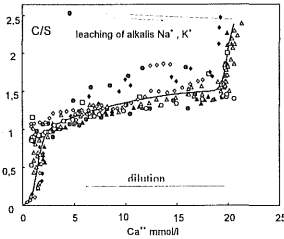


Figure 1: Equilibrium diagram giving C/S ratio as a function of  $Ca^{++}$  concentration in pore solution, after Ref. 2.

The cement paste deterioration reveals a dissolution front of  $Ca(OH)_2$  which moves forward into the pastes with time. In fact, the degradation of cement paste is made of several dissolution fronts depending on the relative solubility of each hydrates. The rate at which these fronts evolve depends not only on the solubility of the hydrates but mainly on the diffusivity of ionic species. The dissolution front of portlandite follows a square root function of time when considering an unidirectional diffusion process (Eq.1):

$$X_d = a \cdot t^{0.5} \quad (1)$$

where  $X_d$  is the penetration depth of portlandite dissolution (mm),  $t$  is the time (years),  $a$  is a constant. For cement pastes,  $a$  ranges between 1 and 5 typically.

The main consequences on the cement paste microstructure are an increase in porosity, a loss of elastic properties and a loss of strength. Figure 2 shows the evolution of the Young's modulus of the material as a function of the pore solution calcium

content. This plot suggests that chemical damage may be represented as a function of the  $Ca^{++}$  content. Over the years, two different kinds of models have been developed to describe the mechanisms of calcium leaching in cement-based materials: the geochemist or chemo-physical approaches and the simplified approaches.

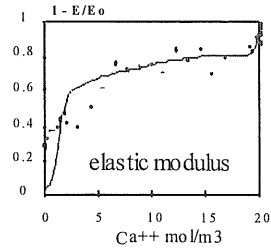


Figure 2: Consequence of calcium leaching of a cement paste on elasticity (obtained by micro-hardness [4]).

The chemo-physical approaches consist in solving the different equations governing the transport of each species in the pore solution. These take into account the intricate thermodynamical equilibrium and can also model the kinetics of dissolution-precipitation of solid phases.

The simplified approach avoids to consider all the elementary chemical mechanisms and focuses on the evolution of one variable only. The leaching prediction is obtained by solving a non-linear diffusion equation. The assumptions are: local equilibrium, water saturation and isothermal conditions. On the basis of these assumptions, Gerard [4] showed that the kinetics of calcium leaching can be determined from the following equation obtained by calculating the mass conservation of calcium:

$$\frac{\partial C_{solid}}{\partial t} \cdot \frac{\partial C}{\partial a} = \text{div}[D(C) \cdot \text{grad}(C)] \quad (2)$$

where  $C_{solid}$  denotes the amount of calcium in the solid phase and  $C$  denotes now (and in the remaining

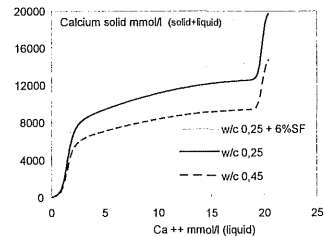


Figure 3: Mathematical relationship used to describe the equilibrium diagram of calcium in hardened cement pastes as a function of the cement chemistry and w/c ratio.

part of the paper) the amount of calcium in the liquid phase. A mathematical relationship for the calcium solid/liquid equilibrium described in Figure 1 was proposed using cement mineralogical data and water to cement ( $w/c$ ) ratio (Fig. 3).

The evolution of the diffusion coefficient  $D$  is also related to the volume fraction of the different solid phases. It varies between that of the virgin material and the diffusion coefficient of calcium in water (when the material is totally cracked).

### 3. SIZE EFFECT TESTS

The experimental program performed consists in residual strength tests: the residual behaviour of mortar beams is obtained after leaching in an aggressive solution [8]. The studied specimens are mortar beams of rectangular cross section. Different sizes of beams have been cast in order to study the size effect: geometrically similar specimens of various height  $D = 80, 160, \text{ and } 320 \text{ mm}$ , of length  $L = 4D$ , and of thickness  $b = 40 \text{ mm}$  kept constant for all the specimens. The length-to-height ratio is  $L/D = 4$  and the span-to-height ratio is  $l/D = 3$ . All specimens were cast with the side of height in the vertical position, using a water-cement ratio of 0.4 and a cement-sand ratio 0.46 (all by weight). The maximal sand grain size is  $d_a = 3 \text{ mm}$ .

The leaching kinetics is a very slow process (a few centimetres per hundred years). In order to collect experimental data in a reasonable period of time, it is necessary to use an accelerated procedure. For this study an ammonium nitrate solution has been selected at a concentration of 480 g/l and kept at 30 °C. The dissolution of portlandite  $\text{Ca(OH)}_2$  is higher than that in pure water: 100 times higher for a OPC (ordinary Portland Cement) paste with a 0.5 water-cement ratio [3]. The beams are immersed into the aggressive solution during different periods of time (28, 56 and 98 days). Only the two lateral sides are exposed in order to have a unidirectional leaching front. The others faces are coated with a silicon resin, so that ammonium nitrate can not penetrate. The leaching depth  $X_d$  is measured by penetration of phenolphthalein [13]. The phenolphthalein reacts with the pH of the pore solution and changes its colour when the pH is about 9. During the degradation of the concrete, the pH goes from 13 to the pH of the external solution. So, phenolphthalein does not measure the maximal degraded depth and an additional microstructural analysis using an electronic microprobe has been carried out in order to correct the measure given by phenolphthalein. The kinetics follows a square root function of time, as follows (time is in days now):

$$X_d = 1,7\sqrt{t} \quad (3)$$

After the chemical degradation tests, the residual mechanical behaviour of the beams is obtained. The specimens are loaded using a three-point bending procedure. All the tests are carried out on the same 100 kN MTS machine. One notch of depth  $D/10$  and thickness 3 mm (same for all specimens) is sawed just before the mechanical test. The tests are notch opening controlled using an MTS extensometer. A second extensometer follows the deflection of a central point of the beam.

A good repeatability between the tests was observed. Figure 4 shows the average responses for different leaching rates for the small beams. The leaching rate  $L_R = 2X_d / b$  influences the mechanical behaviour of beams: the higher the leaching rate, the lower the stiffness and the maximal strength.

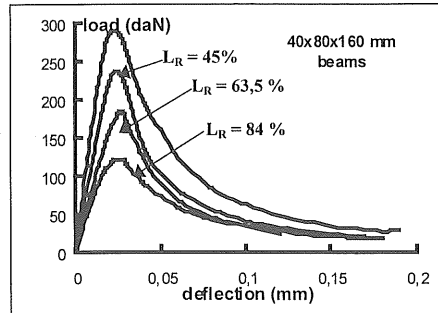


Figure 4: influence of leaching rate  $L_R$  on the structural behaviour, average load - deflection curves for different leaching rates on  $40 \times 80 \times 160 \text{ mm}^3$  beams.

Figures 5 and 6 show the compilation of experimental results, for the three sizes at two different leaching rates (0% and 63.5 % of the beam thickness).  $D_1$  denotes the large size beams,  $D_2$  the medium size beams and  $D_3$  the small size beams.

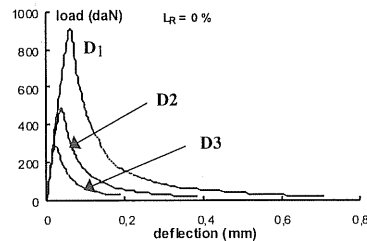


Figure 5: Size effect test prior to leaching.

Let us assume that the material in the degraded zone is homogeneous so that the beam is made by two different materials: a sound zone,  $(40 - 2X_d) \text{ mm}$

thick, and a degraded zone,  $(2X_d)$  mm thick. The global mechanical response of a beam is the sum of the behaviour of two parallel beams: a leached beam and a sound beam. By subtracting the contribution of the average sound beam behaviour in the average global leached beams behaviour, we obtain the response of the average degraded beam behaviour. We used the experiments with a leaching rate of 45% in order to obtain the response of degraded beams (by subtracting that of sound beams) and checked by predicting the responses at the two other leaching rates. Satisfying predictions were obtained [8].

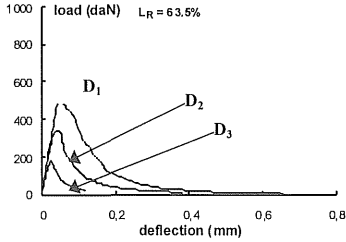


Figure 6: Size effect tests at a leaching rate of 63.5%.

Bazant [1] proposed a procedure to characterise the size effect in beams. The maximal strength is obtained with the formula:

$$\sigma = \frac{3}{2} \frac{Fl}{bD^2} \quad (4)$$

where  $b$  is the thickness of the beam,  $D$  is the height (mm),  $l$  the span (mm), and  $F$  the maximal load (N).  $F$  is obtained for each different sizes. A simple size effect law for concrete and others materials is used:

$$\sigma = \frac{Bf_t'}{\sqrt{1 + D/D_0}} \quad (5)$$

where  $\sigma$  is the maximal strength,  $D$  is the size of the beam (height in this case),  $f_t'$  is the tensile strength of the material,  $D_0$  is a characteristic size which corresponds to a change of failure mechanism between plasticity and fracture, and  $B$  is a material parameter. The fit of this size effect law is shown on Fig. 7. Pure plasticity and pure LEFM (linear elastic fracture mechanics) theoretical responses are also plotted. The larger the beam, the lower the relative strength. A loss of about 20% is measured comparing the two extreme sizes. Moreover, it can be noticed that the mechanical failure of the leached part tends to obey more to fracture mechanics than to plasticity. There is a shift of the experimental points to the right as the material is degraded. A linear regression is used:

$$\frac{1}{\sigma^2} = aD + c \quad (6)$$

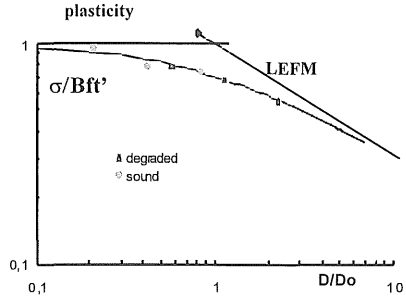


Figure 7: Size effects laws for sound and degraded materials.

#### 4. CONSTITUTIVE MODEL

The mechanical effect of progressive micro-cracking due to external loads is described by a single internal variable which degrades the Young's modulus of the material. The constitutive relations are:

$$\sigma_{ij} = (1 - d)\Lambda_{ijkl}\varepsilon_{kl} \quad (7)$$

where  $\sigma_{ij}$  and  $\varepsilon_{ij}$  are the components of the stress and strain tensors respectively ( $i, j, k, l \in [1, 3]$ ),  $\Lambda_{ijkl}$  are the initial stiffness modulus, and  $d$  is the damage variable. The material is initially isotropic, with  $E_0$  and  $\nu_0$  the initial Young's modulus and Poisson's ratio respectively. Damage is a function of the positive strains which means that it is mainly due to micro cracks opening in mode I. The following scalar called equivalent strain is defined:

$$\tilde{\varepsilon} = \sqrt{\sum_{i=1}^3 \langle \varepsilon_i \rangle_+^2} \quad (8)$$

where  $\langle \cdot \rangle_+$  is the Macauley bracket and  $\varepsilon_i$  are the principal strains. In order to avoid ill-posedness due to strain softening, the mechanical model has to be enriched with an internal length. The non local variable which represents the average of the equivalent strain over the representative volume surrounding each point in the material is defined [11]:

$$\tilde{\varepsilon}(x) = \frac{1}{V_r(x)} \int_{\Omega} \psi(x-s)\tilde{\varepsilon}(s)ds \quad (9)$$

with  $V_r(x) = \int_{\Omega} \psi(x-s)ds$

where  $\Omega$  is the volume of the structure,  $V_r(x)$  is the representative volume at point  $x$ , and  $\psi(x-s)$  is the weight function:

$$\psi(x-s) = \exp\left(-\frac{4|x-s|^2}{l_c^2}\right) \quad (10)$$

$l_c$  the internal length of the non local continuum.  $\bar{\varepsilon}$  is the variable which controls the growth of damage according to the following conditions:

$$F(\bar{\varepsilon}) = \bar{\varepsilon} - \kappa \quad (11)$$

if  $F(\bar{\varepsilon}) = 0$  and  $\dot{F}(\bar{\varepsilon}) = 0$

then  $\begin{cases} d = h(\kappa) \\ \kappa = \bar{\varepsilon} \end{cases}$  with the condition  $\dot{d} \geq 0$

else  $\begin{cases} \dot{d} = 0 \\ \dot{\kappa} = 0 \end{cases}$

$\kappa$  is the softening parameter and takes the largest value of  $\bar{\varepsilon}$  ever reached during the previous loading history at a given time and at the considered point in the medium. Initially  $\kappa = \kappa_0$ , where  $\kappa_0$  is the threshold of damage. The damage evolution law, generically denoted as  $h(\kappa)$  in (11), are those defined by Mazars [9]. In particular, the tensile damage growth is

$$d_t = 1 - \frac{\kappa_0(1-A_t)}{\kappa} - \frac{A_t}{\exp(B_t(\kappa - \kappa_0))} \quad (12)$$

Constants  $A_t$ ,  $B_t$  are model parameters.

The influence of the chemical damage on the mechanical properties of the material may be introduced in the stress – strain relations following several different ways. One method consists in adding a new variable  $V$  in the state equations [4]. This chemically induced damage variable acts as the mechanically induced damage variable. It is an independent contribution to the weakening of the material, which takes a value between zero (for chemically sound material) and one for totally dissolved material. The stress – strain relation is now:

$$\sigma_{ij} = (1-d)(1-V)\Lambda_{ijkl}\dot{\varepsilon}_{kl} - \Lambda_{ijkl}\varepsilon_{kl}(\dot{d} + \dot{V}) \quad (13)$$

$V$  is a function of the concentration  $C$  of calcium in pore solution :

$$V = g(C) \quad (14)$$

where  $g$  is an experimentally determined function.

If one derives the stress – strain relations in a rate format, the following results are obtained:

$$\dot{\sigma}_{ij} = (1-d)(1-V)\Lambda_{ijkl}\dot{\varepsilon}_{kl} - \Lambda_{ijkl}\varepsilon_{kl}(\dot{d} + \dot{V}) \quad (15)$$

If we denote as  $d_m$  and  $d_{ch}$  the part of mechanical and chemical damage in the first formulation respectively, These two relations are identical if

$$(1-d_m - d_{ch}) = (1-d)(1-V) \quad (16)$$

It implies that the cross term  $dV$  is negligible in the right hand-side of this equation. This is true when  $d$  is small and  $V$  is large or conversely. Obviously the differences are also small when these two are small.

In the remaining part of this paper, we will focus attention on the second formulation and examine its calibration and predictive capabilities. The stress – strain laws at different values of chemical damage is shown on Fig. 8.

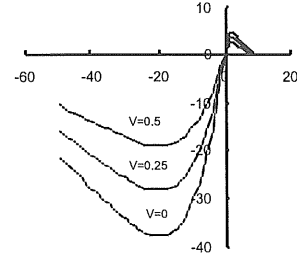


Figure 8: Constitutive law of a concrete as a function of the ageing variable  $V$  (stresses on the vertical axis are in MPa, strains on the horizontal axis are  $m/m 10^{-4}$ ).

## 5. CALIBRATION OF THE MECHANICAL MODEL

A sensitivity analysis has concluded that the constitutive relation is extremely sensitive to the material strength and to the fracture energy [10]. This conclusion is two-sided: on one side such a sensitivity is good for calibration purposes and on the other side, small errors in the calibration may yield a lack of accuracy of predictions. It underlines anyway the need to calibrate the model from experiments especially designed for obtaining the internal length of the materials (for mechanical damage). This is the purpose of the size effect tests depicted in section 3.

We will discuss in this section the calibration of the mechanical model. It has been performed from the size effect test data on sound beams. The model parameters are fitted so as to obtain a satisfactory fit of the load – deflexion curves for the three beam

sizes. A finite element model has been used for this purpose.

One of the difficulties is to calibrate the model parameters in the damage evolution law and the internal length at the same time. Figures 9-10 show two admissible fits which differ completely. The parameters are:

Set 1:

$$l_c = 40\text{mm}, E = 38500\text{MPa},$$

$$A_i = 0.85, B_i = 9000, \kappa_0 = 0.3 \cdot 10^{-5}$$

Set 2:

$$l_c = 7\text{mm}, E = 38500\text{MPa},$$

$$A_i = 0.75, B_i = 3500, \kappa_0 = 0.25 \cdot 10^{-5}$$

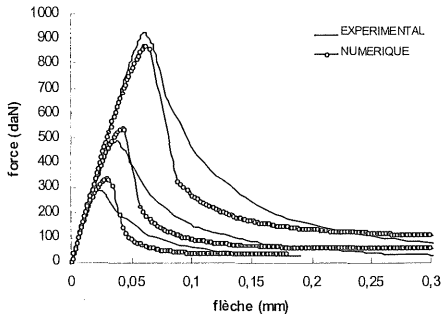


Figure 9: Fit of the mechanical model with the parameter set 1.

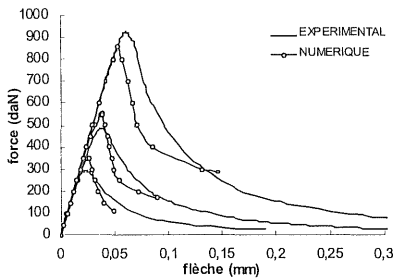


Figure 10: Fit of the mechanical model with the parameter set 2.

Globally these two fits are acceptable. If this was to be true, it would mean that the mechanical model cannot be calibrated objectively because there are several, quite different sets of parameters which provide identical fits. The difference between these two fits ought to be magnified. For this purpose, the size effect method is quite adequate. Each of this fit can be analysed through a subsequent fit of the size effect formula in Eq. (5). Figure 15 shows the result of such interpretation for several quasi-identical fits. We have also reported on this fit bounds (borne sup – borne inf) between which the best fit should be.

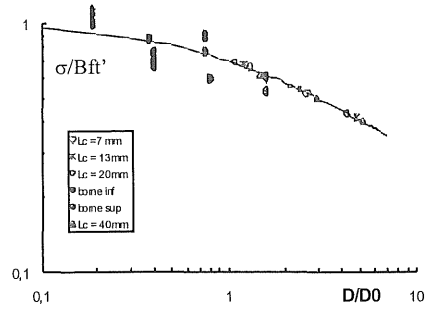


Figure 11: Interpretation of quasi-identical fits on the size effect plot.

The sets of model parameters exhibit, in particular quite different internal lengths. It becomes clear on this figure that the best fit is the one obtained with an internal length equal to 40 mm. It can be also concluded that the optimum fit has not been obtained since it was not possible to place all the computed points of a single set within the experimental bounds. This result shows that it is quite difficult to calibrate the mechanical model. Even if the model prediction provides good results compared to the experimental data, their *extrapolations* to structures of very different sizes will not be accurate because the size effect law is not well fitted.

## 6. PREDICTIONS OF THE RESIDUAL STRENGTH OF LEACHED BEAMS

Since the parameters controlling chemical damage can be fitted independently, it is possible now to compute the predicted responses of the beams at different leaching rates. For this purpose, a diffusion problem is solved first within the beam thickness. Then, the distribution of calcium in the liquid phase at any time can be converted into a distribution of chemical damage. Its average value over the thickness is incorporated into the mechanical model (decrease of Young's modulus) and the load deflexion curve of beams can be computed. Figure

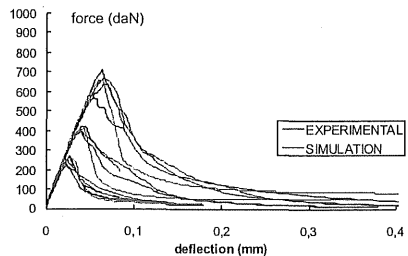


Figure 12: Prediction of the response of leached beams (leaching rate of 45%).

12 shows these predictions for a leaching rate of 45 % and figure 13 shows the same computation at a leaching rate of 64%. The average Young's moduli of the beams have been decreased by 25% and 40% respectively.

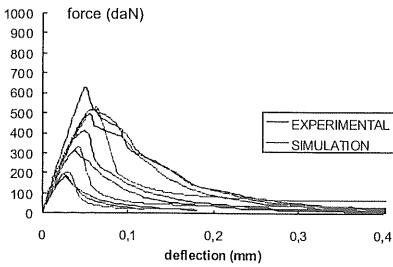


Figure 13: Prediction of the response of leached beams (leaching rate of 64%).

These predictions can be considered to be quite satisfactory. It is again illuminating to examine their accuracy with the help of the size effect plot. Several sets of data can be compared: the experimental one, which is shown on Fig. 15 and the numerical one shown on Fig. 14.

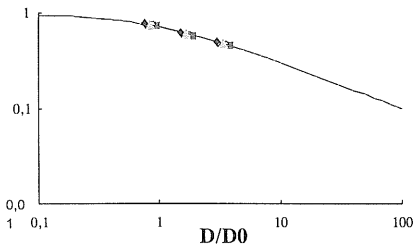


Figure 14: Prediction of the size effect curve at several leaching rates.

The comparisons between Figs. 14 and 15 show that the model is not capable of yielding good predictions of the size effect. The comparison between the experimental data in section 3 for sound and degraded materials and the above figures suggests that the internal length of the material

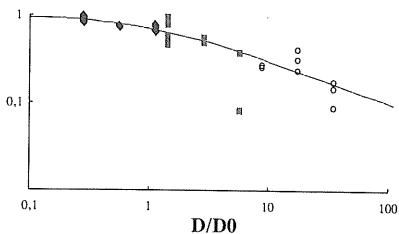


Figure 15: Experimental size effect curve at several leaching rates.

should depend on the state of leaching. Here, the size effect predictions exhibit very small variations between the sound and leached cases, whereas experiments show much larger variations. In order to have better fits, Fig. 7 suggests that the internal length in the mechanical model, at least, should decrease as the chemical degradation proceeds.

## 7. CLOSURE

- A constitutive relation aimed at describing the influence of leaching in concrete and mechanical damage has been studied in this contribution. Sensitivity analyses show that the tensile strength of concrete, the fracture energy and the internal length in the non local mechanical damage model are extremely influent on the life-time of bending beams subjected to a fixed displacement at mid-span and to leaching.

- Size effect experiments have been presented. These data show that the material becomes more brittle upon leaching.

- The calibration of the mechanical model on load - deflexion curves is very delicate and may yield several set of model parameters with the same level of accuracy. The interpretation of the computations with the size effect law acts as a magnifying tool which enables to distinguish which set of data is the more appropriate.

- The comparison between the prediction of the response of beams at several leaching rates and the experiments is of a rather good quality. Unfortunately, predictions and experiments fit size effect laws that are quite different. It follows that the extrapolation of the computations to large size structures is quite delicate because accuracy will be lost. In order to correct this feature, the internal length in the mechanical model should depend on the state of leaching.

## 8. REFERENCES

- [1] Bazant Z., Planas J., Fracture and Size Effect in Concrete and Other Quasibrittle Materials, CRC Press, 1998.
- [2] Berner U.R., Evolution of Pore Water Chemistry During Degradation of Cement in a Radioactive Waste Repository Environment, Waste Management, vol. 12, pp 201-219, 1992.
- [3] Carde, C., Characterization and modeling of the alteration of material properties due to leaching of cement-based materials, Ph.D thesis, Université Paul Sabatier, Toulouse, France, 218p. (in French), 1996.
- [4] Gérard, B., Contribution of the mechanical, chemical, and transport couplings in the long-term behavior of radioactive waste repository structures, Ph.D. Thesis, Département de Génie Civil, Université Laval, Québec,

- Canada / École Normale Supérieure de Cachan, France, 278p. (in French), 1996.
- [5] Gérard B., Pijaudier-Cabot G. and La Borderie C., Coupled Diffusion-Damage Modelling and the Implications on Failure due to Strain Localisation, *Int. J. Solids & Structures*, Vol. 35, pp. 4105-4120, 1998
- [6] Goncalves A., Rodrigues X., "The Resistance of Cement to Ammonium Nitrate Attack", *Durability of concrete*, 2<sup>nd</sup> International Conference, Montreal, Canada, 1991.
- [7] Kamali S., Identification de la loi de comportement mécanique d'un mortier altéré par le nitrate d'ammonium, Master thesis, ENS Cachan, 1999.
- [8] Le Bellégo C., Gérard B., and Pijaudier-Cabot G., Chemomechanical Effects in Mortar Beams Subjected to Water Hydrolysis, *J. Engrg. Mech. ASCE*, Vol. 126, pp. 266-272, 2000.
- [9] Mazars J., Application de la mécanique de l'endommagement au comportement non linéaire et à la rupture de béton de structure, thèse de Doctorat d'Etat, Université Paris VI, France, 1984.
- [10] Molez L., Gérard B., and Pijaudier-Cabot G., Couplage endommagement mécanique – endommagement chimique : étude d'un modélisation numérique, *Revue Française de Génie Civil*, Vol. 2, pp. 481-504, 1998.
- [11] Pijaudier-Cabot G. and Bazant Z.P., Nonlocal Damage Theory, *J. of Engrg. Mech.*, ASCE, Vol. 113, pp. 1512-1533, 1987.
- [12] Schneider U., Nägele E., Dumat F., Holst S., « Der Einfluss Mechanischer Spannungen auf den Korrosionswiderstand Zementgebundener Baustoffe », *DAFStB Heft 429*, Beuth Verlag GmbH, Berlin / Köln, Germany, 1992 (in German).
- [13] Schneider, Chen, The Chemomechanical Effect and the Mechanochemical Effect on High-Performance Concrete Subjected to Stress Corrosion, *Cement and Concrete Research*, vol. 28, n°4, pp. 509-522, 1998.
- [14] Schneider U., Chen S. W., Behavior of High-Performance Concrete under Ammonium Nitrate Solution and Sustained Load, *ACI Materials Journal*, vol.96, n°1, pp 47-51, 1999.